DOA Estimation for Coherently Distributed Sources Considering Circular and Noncircular Signals in Massive MIMO Systems

Liangtian Wan, *Member, IEEE*, Guangjie Han, *Member, IEEE*, Jinfang Jiang, Joel J. P. C. Rodrigues, *Senior Member, IEEE*, Naixing Feng, and Tong Zhu

***Abstract*—In mobile communication, the signal that a base station received cannot be regarded as a point source anymore because of the multipath propagation. A distributed source model is more suitable for the realistic scenarios. In this paper, an approach of direction-of-arrival (DOA) estimation is proposed for coherently distributed (CD) sources consisting of circular and noncircular signals in a massive or large-scale multiple-input multiple-output system. The noncircular characteristic can improve the performance of DOA estimation. However, most algorithms are not suitable for DOA estimation where circular and noncircular signals coexist. Based on the analysis of constraint conditions satisfied by the steering vector of mixed signals, a multiple signal classification (MUSIC) like approach is proposed for the DOA estimation of CD sources consisting of circular and noncircular signals. On the conditions of low signal-to-noise ratio, small snapshot numbers, and large source numbers, the pseudo-peaking may appear. This phenomenon has been analyzed, and a modified MUSIC-like approach is proposed. Simulation results demonstrate that both two proposed algorithms can estimate more sources than the number of sensors. The estimation performances of the two proposed algorithms outperform the traditional MUSIC algorithm.**

***Index Terms*—Circular and noncircular signals, coherently distributed (CD) sources, direction-of-arrival (DOA) estimation, massive multiple-input multiple-output (MIMO).**

I. Introduction

MASSIVE or large-scale multiple-input multiple-output (MIMO) techniques can tremendously improve the performance of wireless networks. In the future communication architectures, the fifth generation (5G) will be a paradigm shift that includes very high carrier frequencies with massive andwidths, extreme base station (BS) and device densities, and unprecedented numbers of antennas [1]. As a key technology of 5G, massive MIMO can offer higher data rates, enhanced link reliability, and potential power savings. Massive MIMO BSs are equipped with a very large number of antennas (possibly tens to hundreds of antennas) and simultaneously communicate with multiple users on the same frequency band [2]. However, the angular spread effect of electromagnetic wave propagation cannot be ignored due to the multipath channels in many applications, e.g., radar, sonar, and mobile communication. If the transmitted signals of user equipment are regarded as point sources, the performance of massive MIMO systems will degrade significantly. Thus, a spatial distributed source model consisting of hundreds of point sources was introduced [3]. Generally, the reflection and refraction in a channel cause angular spread. The distributed sources can be categorized into incoherently distributed (ID) and coherently distributed (CD) sources corresponding to rapidly and slowly time-varying channels, respectively [4]. The first comprehensive survey on spatial distributed source was reported in [5], where a distributed source model has been systemically elaborated. The multiple signal classification (MUSIC) algorithm [6] was employed to estimate the direction-of-arrival (DOA) [7], [8] of the distributed source model in [5].

For CD sources, many DOA estimation algorithms have been proposed [9]–[14]. Two distributed source models (parametric and nonparametric) were considered in [9]. A 2-D DOA estimation problem was solved by a MUSIC-based method for the parametric model, and a direct method under a nonparametric model was also investigated. A two-step procedure [10] was proposed to decouple the estimation of DOA from that of the angular spread, and the extended invariance principle is combined with the covariance matching algorithm. Estimating signal parameters via the rotational invariance technique (ESPRIT) based algorithm has been proposed for CD source estimation [11]. However, the extension width was estimated by the distributed source parameter estimator based on spectrum searching. A sparse representation approach combined with total least squares-ESPRIT was proposed for the CD source estimation [12]. However, its computational complexity was also tremendous. For the 2-D DOA estimation, an algorithm named as sequential 1-D searching was proposed based on uniform circular arrays [13]. However, a 1-D searching was needed as well. Based on three parallel uniform linear

Manuscript received December 15, 2014; revised April 25, 2015 and June 7, 2015; accepted June 10, 2015. Date of publication July 7, 2015; date of current version March 10, 2017. This work was supported in part by Qing Lan Project, by the National Science Foundation of China under Grants 61401147 and 61201410, and by the Natural Science Foundation of JiangSu Province of China (No. BK20140248).

L. Wan, G. Han, and J. Jiang are with the Department of Information and Communication Systems, Hohai University, Changzhou 213022, China (e-mail: wanliangtian1@163.com; hanguangjie@gmail.com; jiangjinfang1989@gmail.com).

J. J. P. C. Rodrigues is with the Instituto de Telecomunicações, University of Beira Interior, 6201-001 Covilhã, Portugal (e-mail: joeljr@ieee.org).

N. Feng is with the Institute of Electromagnetics and Acoustics, Xiamen University, Xiamen 361005, China (e-mail: fengnaixing@gmail.com).

T. Zhu is with Tianjin Institute of Computing Technology, Tianjin 300000, China (e-mail: zhutongheu@gmail.com).

Digital Object Identifier 10.1109/JSYST.2015.2445052

arrays (ULAs), the propagator method was proposed for the 2-D CD source estimation [14].

For the DOA estimation of the noncircular signals, e.g., binary phase shift keying (BPSK) signal and amplitude modulation signal, their unconjugated covariance matrix is not equal to zero, which can be implemented to improve the DOA estimation performance. The NC-MUSIC algorithm was first proposed in 1998 [15]. The real-valued ESPRIT algorithm was introduced to estimate the DOAs of noncircular signals with a rule hexagonal array, and the Cramer–Rao lower bound (CRB) was derived [16]. The noncircular asymptotically minimum variance algorithm was proposed in [17], which can approximate the CRB. However, its computational complexity is tremendous because of multidimensional parameter searching. The CRBs for the noncircular signals with additive white Gaussian noise (AWGN) [18] and known color noise [19] were derived. Based on an ESPRIT-like algorithm, a 2-D DOA estimation of CD noncircular sources was proposed in [20].

For a massive MIMO system, an ESPRIT-like algorithm was proposed for the DOA estimation of ID sources [21]. Based on the unitary transformation, a low-complexity 2-D DOA estimation algorithm was proposed, and the CRB was derived [22]. Based on the ESPRIT algorithm, the 2-D DOA estimation was achieved in the massive MIMO system. Moreover, the capacity of the 2-D massive MIMO system was studied [23]. A two-stage low-complexity DOA estimation scheme, in which two MUSIC algorithms are performed for estimating, respectively, the elevation and azimuth angles of the impinging sources, was proposed in [22].

To the best of our knowledge, there have been few reports about the DOA estimation for CD sources consisting of circular and noncircular signals. In this paper, a MUSIC-like DOA estimation algorithm is proposed, which can estimate circular and noncircular signals synchronously. The pseudopeaking may appear in low signal-to-noise ratio (SNR) and other imperfect conditions. The reason leading to this phenomenon will be analyzed, and a modified MUSIC-like DOA estimation algorithm is proposed. Moreover, both of the two algorithms can estimate more sources than the number of sensors.

This paper is organized as follows. The generalized MUSIC algorithm for CD sources is introduced in Section II. Two MUSIC-like algorithms are proposed in Section III. Several issues about the pseudopeaking are discussed in Section IV. The simulation results are shown and analyzed in Section V. The conclusion is drawn in Section VI.

Notation: In this paper, operators $(\cdot)^*$, $(\cdot)^{\mathrm{T}}$, $(\cdot)^{\mathrm{H}}$, and $E\{\cdot\}$ denote conjugate, transpose, conjugate transpose, and expectation, respectively. The boldface uppercase letters and boldface lowercase letters denote matrices and column vectors, respectively. The operator $\|\|_{\mathrm{F}}$ stands for the Frobenius norm of a matrix. $\mathrm{diag}\{z_1, z_2\}$ stands for a diagonal matrix whose diagonal entries are z_1 and z_2. $\mathbf{I}_M$ stands for an $M \times M$ identity matrix.

II. Generalized MUSIC Algorithm

It is assumed that q uncorrelated narrowband CD sources transmitted by UTs impinge on the BSs equipped with a ULA in a massive MIMO system. A ULA consists of M sensors, and the distance among adjacent sensors is d. The received data vector $\mathbf{x}(t)$ at time t is given by

$$\mathbf{x}(t) = \mathbf{A}\mathbf{s}(t) + \mathbf{n}(t) \tag{1}$$

where $\mathbf{A} = [\mathbf{a}_1, \mathbf{a}_2, \ldots, \mathbf{a}_q]$ is the $M \times q$ generalized steering matrix, $\mathbf{s}(t) = [s_1(t), s_2(t), \ldots, s_q(t)]^{\mathrm{T}}$ is the $q \times 1$ signal vector, and $\mathbf{n}(t)$ is the $M \times 1$ AWGN vector with zero means and variance σ_n^2. $\mathbf{a}_i = \mathbf{a}(\theta_i, \sigma_{\theta_i})$ is the generalized steering vector of the ith CD source, which is expressed as

$$\mathbf{a}(\theta, \sigma_\theta) = \int \mathbf{c}(\theta)\rho(\theta, \sigma_\theta)d\theta \tag{2}$$

where θ and σ_θ are the central DOA and the angular spread, respectively. $\rho(\theta, \sigma_\theta)$ and $\mathbf{c}(\theta)$ denote the probability density function (PDF) of angular spread and the $M \times 1$ complex exponential vector, respectively.

For the 1-D signal model of CD source, the PDF of angular spread $\rho(\theta, \sigma_\theta)$ is normally uniform or Gaussian distribution; thus, we have

$$a_k(\mu) = [\mathbf{a}(\theta, \sigma_\theta)]_k \approx [\mathbf{c}(\theta)]_k [\mathbf{g}(\theta, \sigma_\theta)]_k \tag{3}$$

where $[\mathbf{c}(\theta)]_k$ is the complex exponential term. Because the PDF of angular spread is symmetrical, $[\mathbf{g}(\theta, \sigma_\theta)]_k$ is a real number, $k = 1, 2, \ldots, M$. $[\mathbf{c}(\theta)]_k$ is given by

$$[\mathbf{c}(\theta)]_k = \exp\left(j\left(\frac{2\pi}{\lambda}\right)d(k-1)\sin\theta\right). \tag{4}$$

For the CD source following uniform distribution, the PDF of angular spread is given by:

$$\rho(\theta, \sigma_\theta) = \begin{cases} \frac{1}{2\sigma_\theta}, & |\theta - \bar{\theta}| \le \sigma_\theta \\ 0, & |\theta - \bar{\theta}| > \sigma_\theta \end{cases} \tag{5}$$

where $\bar{\theta}$ is the angular range of the different incident signals in one CD source. The corresponding $[\mathbf{g}(\theta, \sigma_\theta)]_k$ is given by

$$[\mathbf{g}(\theta, \sigma_\theta)]_k = \frac{\sin\left((k-1)\sigma_\theta\right)}{(k-1)\sigma_\theta}. \tag{6}$$

For the CD source following Gaussian distribution, the PDF of angular spread is given by

$$\rho(\theta, \sigma_\theta) = \frac{1}{\sqrt{2\pi\sigma_\theta^2}}\exp\left(-\frac{(\theta - \bar{\theta})}{2\sigma_\theta^2}\right) \tag{7}$$

then the corresponding $[\mathbf{g}(\theta, \sigma_\theta)]_k$ is given by

$$[\mathbf{g}(\theta, \sigma_\theta)]_k = \exp\left(-\frac{(k-1)}{2}\sigma_\theta^2\right). \tag{8}$$

According to received data vector $\mathbf{x}(t)$, the covariance matrix of $\mathbf{x}(t)$ is expressed as

$$\mathbf{R} = \mathrm{E}\left\{\mathbf{x}(t)\mathbf{x}^H(t)\right\} = \mathbf{A}\mathbf{R}_{\mathrm{S}}\mathbf{A}^H + \sigma_n^2\mathbf{I}_M \tag{9}$$

where $\mathbf{R}_{\mathrm{S}}$ is the signal covariance matrix of CD sources.

The singular value decomposition of $\mathbf{R}$ is given by

$$\mathbf{R} = \mathbf{U}_{\mathrm{S}}\mathbf{\Sigma}_{\mathrm{S}}\mathbf{U}_{\mathrm{S}}^{\mathrm{H}} + \mathbf{U}_{\mathrm{N}}\mathbf{\Sigma}_{\mathrm{N}}\mathbf{U}_{\mathrm{N}}^{\mathrm{H}} \tag{10}$$

where the column vectors of $\mathbf{U}_{\mathrm{S}}$ and $\mathbf{U}_{\mathrm{N}}$ are constructed by the singular vectors corresponding to the q largest singular values and $M-q$ other singular values, respectively. The entries of diagonal matrices $\mathbf{\Sigma}_{\mathrm{S}}$ and $\mathbf{\Sigma}_{\mathrm{N}}$ are constructed by the q largest singular values and $M-q$ other singular values, respectively.

Since CD sources are uncorrelated with each other and then $\mathbf{R}_{\mathrm{S}}$ is a nonsingular matrix, we have

$$\mathbf{U}_{\mathrm{N}}^{\mathrm{H}}\mathbf{a}\left(\theta_i, \sigma_{\theta_i}\right) = 0,\ i = 1, 2 \ldots, q. \tag{11}$$

According to the structure of the steering vector given in (3), $\mathbf{a}(\theta_i, \sigma_{\theta_i})$ is the function of incident signal θ_i and angular spread σ_{θ_i}. Obviously, when $\theta \neq \theta_i$, $\sigma_\theta \neq \sigma_{\theta_i}$, $i = 1, 2, \ldots, q$, we have $\mathbf{a}^{\mathrm{H}}(\theta, \sigma_{\theta_i})\mathbf{U}_{\mathrm{N}} \neq \mathbf{0}$. Based on the orthogonality between signal and noise subspace, the conventional MUSIC estimator [6] involves minimizing its null-spectrum function as follows:

$$f\left(\theta, \sigma_{\theta_i}\right) = \left\|\mathbf{a}^{\mathrm{H}}\left(\theta, \sigma_{\theta_i}\right)\mathbf{U}_{\mathrm{N}}\right\|_{\mathrm{F}} = \mathbf{a}^{\mathrm{H}}\left(\theta, \sigma_{\theta_i}\right)\mathbf{U}_{\mathrm{N}}\mathbf{U}_{\mathrm{N}}^{\mathrm{H}}\mathbf{a}\left(\theta, \sigma_{\theta_i}\right). \tag{12}$$

If the PDF of angular spread is identical and known *a priori* such as (5) and (7), then we can obtain the closed expression of generalized steering vector $\mathbf{a}(\theta_i, \sigma_{\theta_i})$. When $\theta = \theta_i$, $\sigma_\theta = \sigma_{\theta_i}$, $i = 1, 2, \ldots, q$, (12) would reach the minimum. We can obtain these DOAs of q incident signals by spectrum peaking searching. This is the fundamental principle of MUSIC as mentioned previously. Generally, the reciprocal of the spatial spectrum given in (12) is usually adopted and can be expressed as

$$f(\theta, \sigma_\theta) = \frac{1}{\mathbf{a}^{\mathrm{H}}(\theta, \sigma_\theta)\hat{\mathbf{U}}_{\mathrm{N}}\hat{\mathbf{U}}_{\mathrm{N}}^{\mathrm{H}}\mathbf{a}(\theta, \sigma_\theta)} \tag{13}$$

where $\hat{\mathbf{U}}_{\mathrm{N}}$ is the estimator of noise subspace. This is the generalized MUSIC algorithm, which needs the two-parameter searching for CD sources.

In practical situations, the theoretical array covariance matrix $\mathbf{R}$ given in (9) is unavailable, and it is usually estimated by

$$\hat{\mathbf{R}} = \frac{1}{L}\sum_{t=1}^{L}\mathbf{x}(t)\mathbf{x}^{\mathrm{H}}(t). \tag{14}$$

In order to simplify the derivation of the expression given in equations as follows, angular spread parameter σ_θ is omitted.

III. DOA Estimation for Circular Signals and Noncircular Signals

For a noncircular signal s, it holds that [24]

$$\mathrm{E}\left[\mathbf{s}(t)\mathbf{s}(t)\right] = \rho \mathrm{e}^{j\beta}\mathrm{E}\left[s(t)s^*(t)\right] \tag{15}$$

in which β is the noncircularity phase, ρ is the noncircularity rate, $\rho = 1$ for the maximal noncircularity rated signal, and $0 < \rho < 1$ for the common noncircularity rated signal.

Signal vector $\mathbf{s}(t)$ consists of q signals, its unconjugated covariance matrix $\mathbf{R}'_{\mathrm{S}}$ is defined as

$$\begin{aligned}\mathbf{R}'_{\mathrm{S}} &= \mathrm{E}\left[\mathbf{s}(t)\mathbf{s}^{\mathrm{T}}(t)\right] \\ &= \mathrm{diag}\left\{\mathrm{E}\left[s_1(t)s_1(t)\right], \mathrm{E}\left[s_2(t)s_2(t)\right], \ldots, \mathrm{E}\left[s_q(t)s_q(t)\right]\right\} \\ &= \mathrm{diag}\left\{\rho_1 \mathrm{e}^{\mathrm{j}\beta_1}\mathrm{E}\left[s_1(t){s_1}^*(t)\right]\right. \\ &\qquad \left.\times \rho_2 \mathrm{e}^{\mathrm{j}\beta_2}\mathrm{E}\left[s_2(t){s_2}^*(t)\right], \ldots, \rho_q \mathrm{e}^{\mathrm{j}\beta_q}\mathrm{E}\left[s_q(t){s_q}^*(t)\right]\right\} \\ &\triangleq \mathbf{PBR}_{\mathrm{S}}\end{aligned} \tag{16}$$

where $\mathbf{P}$ is a diagonal matrix, whose diagonal entries are the non circularity rates of q signals, and it is defined as $\mathbf{P} = \mathrm{diag}\{\rho_1, \rho_2, \ldots, \rho_q\}$. $\mathbf{B}$ is a diagonal matrix, whose diagonal entries are the noncircularity phases of q signals, and it is defined as $\mathbf{B} = \mathrm{diag}\{\exp(\mathrm{j}\beta_1), \exp(\mathrm{j}\beta_2), \ldots, \exp(\mathrm{j}\beta_q)\}$. In particular, when the q signals are all maximal noncircularity rated signals, we have $\mathbf{P} = \mathbf{I}_q$. When the q signals are all circular signals, we have $\mathbf{R}'_{\mathrm{S}} = \mathbf{0}$. It can be seen from (16) that the information of the noncircular signal contained in unconjugated covariance matrix $\mathbf{R}'_{\mathrm{S}}$ is related to signal covariance matrix $\mathbf{R}_{\mathrm{S}}$ via noncircularity rate matrix $\mathbf{P}$ and noncircularity phase matrix $\mathbf{B}$.

According to (1) and (16), the unconjugated covariance matrix $\mathbf{R}'$ of received data vector $\mathbf{x}(t)$ is expressed as

$$\begin{aligned}\mathbf{R}' &= \mathrm{E}\left[\mathbf{x}(t)\mathbf{x}(t)\right] = \mathbf{A}\mathbf{R}'_{\mathrm{S}}\mathbf{A}^{\mathrm{T}} + \mathrm{E}\left[\mathbf{n}(t)\mathbf{n}^{\mathrm{T}}(t)\right] \\ &= \mathbf{APBR}_{\mathrm{S}}\mathbf{A}^{\mathrm{T}}.\end{aligned} \tag{17}$$

In practical situations, similarly with the maximum likelihood estimator given in (14), the unconjugated covariance matrix $\mathbf{R}'$ is estimated by

$$\hat{\mathbf{R}}' = \frac{1}{L}\sum_{t=1}^{L}\mathbf{x}(t)\mathbf{x}^{\mathrm{T}}(t). \tag{18}$$

In order to utilize the noncircular characteristic of incident signals, i.e., the information contained in unconjugated covariance matrix $\mathbf{R}'$, equation $\mathbf{R}'_{\mathrm{S}} = \mathbf{PBR}_{\mathrm{S}}$ is used to connect unconjugated covariance matrix $\mathbf{R}'$ and covariance matrix $\mathbf{R}$ via noncircularity rate and noncircularity phase. Thus, an extended received data vector $\mathbf{y}(t)$ is given by

$$\mathbf{y}(t) = \begin{bmatrix}\mathbf{x}(t) \\ \mathbf{x}^*(t)\end{bmatrix}. \tag{19}$$

Then, the covariance matrix $\mathbf{R}_{\mathbf{y}}$ of the extended received data vector $\mathbf{y}(t)$ is expressed as

$$\begin{aligned}\mathbf{R}_{\mathbf{y}} &= \mathrm{E}\left[\mathbf{y}(t)\mathbf{y}^{\mathrm{H}}(t)\right] \\ &= \begin{bmatrix}\mathbf{A}\mathbf{R}_{\mathrm{S}}\mathbf{A}^{\mathrm{H}} & \mathbf{A}\mathbf{R}'_{\mathrm{S}}\mathbf{A}^{\mathrm{T}} \\ \left(\mathbf{A}\mathbf{R}'_{\mathrm{S}}\mathbf{A}^{\mathrm{T}}\right)^* & \left(\mathbf{A}\mathbf{R}_{\mathrm{S}}\mathbf{A}^{\mathrm{H}}\right)^*\end{bmatrix} + \sigma_{\mathrm{n}}^2\mathbf{I}_{2M}.\end{aligned} \tag{20}$$

Based on $\mathbf{R}'_{\mathrm{S}} = \mathbf{PBR}_{\mathrm{S}}$, (20) can be rewritten as

$$\begin{aligned}\mathbf{R}_{\mathbf{y}} &= \begin{bmatrix}\mathbf{A}\mathbf{R}_{\mathrm{S}}\mathbf{A}^{\mathrm{H}} & \mathbf{APBR}_{\mathrm{S}}\mathbf{A}^{\mathrm{T}} \\ \left(\mathbf{APBR}_{\mathrm{S}}\mathbf{A}^{\mathrm{T}}\right)^* & \left(\mathbf{A}\mathbf{R}_{\mathrm{S}}\mathbf{A}^{\mathrm{H}}\right)^*\end{bmatrix} + \sigma_{\mathrm{n}}^2\mathbf{I}_{2M} \\ &= \begin{bmatrix}\mathbf{A} & -\mathbf{A} \\ \mathbf{A}^*\mathbf{B}^* & \mathbf{A}^*\mathbf{B}^*\end{bmatrix}\begin{bmatrix}\frac{\mathbf{I}_M+\mathbf{P}}{2}\mathbf{R}_{\mathrm{S}} & \mathbf{0} \\ \mathbf{0} & \frac{\mathbf{I}_M-\mathbf{P}}{2}\mathbf{R}_{\mathrm{S}}\end{bmatrix} \\ &\quad \times \begin{bmatrix}\mathbf{A} & -\mathbf{A} \\ \mathbf{A}^*\mathbf{B}^* & \mathbf{A}^*\mathbf{B}^*\end{bmatrix}^H + \sigma_n^2\mathbf{I}_{2M}.\end{aligned} \tag{21}$$

There exist two cases: one is that only maximal noncircularity rated signals exist in incident signals. The other is that maximal noncircularity rated and circular signals coexist.

A. DOA Estimation for Maximal Noncircularity Rated Signals

The noncircularity rated matrix $\mathbf{P}$ of the maximal noncircularity rated signals satisfies

$$\mathbf{P} = \mathbf{I}_q. \tag{22}$$

We define the extended manifold matrix $\mathbf{A}_{\mathrm{nc}}$ as

$$\begin{aligned}\mathbf{A}_{\mathrm{nc}} &\triangleq \begin{bmatrix}\mathbf{A} \\ \mathbf{A}^*\mathbf{B}^*\end{bmatrix} \\ &= [\mathbf{a}_{\mathrm{nc}-1}(\theta,\beta), \mathbf{a}_{\mathrm{nc}-2}(\theta,\beta), \ldots, \mathbf{a}_{\mathrm{nc}-q}(\theta,\beta)]\end{aligned} \tag{23}$$

where $\mathbf{a}_{\mathrm{nc}-i}(\theta,\beta)$ is the extended steering vector. It contains angular parameter θ and noncircularity phase parameter β and can be expressed as

$$\mathbf{a}_{\mathrm{nc}-i} = \begin{bmatrix}\mathbf{a}_i(\theta) \\ \mathrm{e}^{-j\beta_i}\mathbf{a}_i^*(\theta)\end{bmatrix}, i = 1, 2, \ldots, q. \tag{24}$$

Then, the covariance matrix $\mathbf{R}_{\mathbf{y}}$ of the extended array can be given by

$$\mathbf{R}_{\mathbf{y}} = \mathbf{A}_{\mathrm{nc}}\mathbf{R}_{\mathrm{S}}\mathbf{A}_{\mathrm{nc}}^{\mathrm{H}} + \sigma_n^2\mathbf{I}_{2M}. \tag{25}$$

Compared with (9), it can be seen that $\mathbf{R}_{\mathbf{y}}$ has the same form as the covariance matrix $\mathbf{R}$ in the MUSIC algorithm. The extended manifold matrix $\mathbf{A}_{\mathrm{nc}}$ corresponds to manifold matrix $\mathbf{A}$. However, from $\mathbf{R}$ to $\mathbf{R}_{\mathbf{y}}$, the dimension is extended from $M \times M$ to $2M \times 2M$. Thus, the MUSIC algorithm can be used to estimate the DOA of incident signals with high accuracy. The eigenvalue decomposition (EVD) of $\mathbf{R}_{\mathbf{y}}$ is expressed as

$$\begin{aligned}\mathbf{R}_{\mathbf{y}} &= \mathbf{U}_{\mathrm{S}}\mathbf{\Sigma}_{\mathrm{S}}\mathbf{U}_{\mathrm{S}}^{\mathrm{H}} + \mathbf{U}_{\mathrm{N}}\mathbf{\Sigma}_{\mathrm{N}}\mathbf{U}_{\mathrm{N}}^{\mathrm{H}} \\ &= \mathbf{U}_{\mathrm{S}}\mathbf{\Sigma}_{\mathrm{S}}\mathbf{U}_{\mathrm{S}}^{\mathrm{H}} + \sigma_{\mathrm{n}}^2\mathbf{U}_{\mathrm{N}}\mathbf{U}_{\mathrm{N}}^{\mathrm{H}}\end{aligned} \tag{26}$$

where $\mathbf{U}_{\mathrm{S}}$ is the eigenmatrix of $\mathbf{R}_{\mathbf{y}}$ corresponding to the q largest eigenvalues spanning signal subspace. Similarly as $\mathbf{U}_{\mathrm{S}}$, $\mathbf{U}_{\mathrm{N}}$ is the eigenmatrix of $\mathbf{R}_{\mathbf{y}}$ corresponding to $2M - q$ small eigenvalues, which spans noise subspace. Based on the principle of the MUSIC algorithm, the extended manifold matrix $\mathbf{A}_{\mathrm{nc}}$ is orthogonal to the noise subspace, i.e.,

$$\mathbf{A}_{\mathrm{nc}}^{\mathrm{H}}\mathbf{U}_{\mathrm{N}} = \mathbf{0}. \tag{27}$$

Thus, the spatial spectrum function is given by

$$f(\theta,\beta) = \left\|\mathbf{a}_{\mathrm{nc}}^{\mathrm{H}}(\theta,\beta)\mathbf{U}_{\mathrm{N}}\right\|_{\mathrm{F}} = \mathbf{a}_{\mathrm{nc}}^{\mathrm{H}}(\theta,\beta)\mathbf{U}_{\mathrm{N}}\mathbf{U}_{\mathrm{N}}^{\mathrm{H}}\mathbf{a}_{\mathrm{nc}}(\theta,\beta). \tag{28}$$

According to (24), $\mathbf{a}_{\mathrm{nc}}$ can be written as two partitioned matrix; thus, noise eigenmatrix $\mathbf{U}_{\mathrm{N}}$ can be partitioned into two block matrices

$$\mathbf{U}_{\mathrm{N}} = \begin{bmatrix}\mathbf{U}_{\mathrm{N1}} \\ \mathbf{U}_{\mathrm{N2}}\end{bmatrix}. \tag{29}$$

Substituting (24) and (29) into (28), we have

$$\begin{aligned}f(\theta,\beta) &= \left\|\mathbf{a}^{\mathrm{H}}(\theta)\mathbf{U}_{\mathrm{N1}} + \mathrm{e}^{j\beta}\mathbf{a}^{\mathrm{T}}(\theta)\mathbf{U}_{\mathrm{N2}}\right\|_{\mathrm{F}} \\ &= \mathbf{a}^{\mathrm{H}}(\theta)\mathbf{U}_{\mathrm{N1}}\mathbf{U}_{\mathrm{N1}}^{\mathrm{H}}\mathbf{a}(\theta) + \mathbf{a}(\theta)^{\mathrm{H}}\mathbf{U}_{\mathrm{N2}}\mathbf{U}_{\mathrm{N2}}^{\mathrm{H}}\mathbf{a}(\theta) \\ &\quad + \mathrm{e}^{j\beta}\mathbf{a}^{\mathrm{T}}(\theta)\mathbf{U}_{\mathrm{N2}}\mathbf{U}_{\mathrm{N1}}^{\mathrm{H}}\mathbf{a}(\theta) + \mathrm{e}^{-j\beta}\mathbf{a}^{\mathrm{H}}(\theta)\mathbf{U}_{\mathrm{N1}}\mathbf{U}_{\mathrm{N2}}^{\mathrm{H}}\mathbf{a}^*(\theta).\end{aligned} \tag{30}$$

From (30), it can be seen that spatial spectrum function $f(\theta,\beta)$ is not only the function of angular parameter θ but also the function of noncircularity phase parameter β. In order to reduce the computational complexity of parameter searching in (30), the dimension of the unknown parameter in (30) should be reduced. The essence of dimension reduction is that angular parameter θ and noncircularity phase parameter β can make spatial spectrum function $f(\theta,\beta)$ reach the extremum, i.e., the partial derivative of $f(\theta,\beta)$ with respect to θ and β is equal to zero. Thus, we have

$$\begin{aligned}\frac{\partial f(\theta,\beta)}{\partial\beta} &= \mathrm{j}\mathrm{e}^{\mathrm{j}\beta}\mathbf{a}^{\mathrm{T}}(\theta)\mathbf{U}_{\mathrm{N2}}\mathbf{U}_{\mathrm{N1}}^{\mathrm{H}}\mathbf{a}(\theta) \\ &\quad - \mathrm{j}\mathrm{e}^{-\mathrm{j}\beta}\mathbf{a}^{\mathrm{H}}(\theta)\mathbf{U}_{\mathrm{N1}}\mathbf{U}_{\mathrm{N2}}^{\mathrm{H}}\mathbf{a}^*(\theta) = 0\end{aligned} \tag{31}$$

i.e.,

$$\mathrm{e}^{\mathrm{j}\beta} = \pm\frac{\mathbf{a}^{\mathrm{H}}(\theta)\mathbf{U}_{\mathrm{N1}}\mathbf{U}_{\mathrm{N2}}^{\mathrm{H}}\mathbf{a}^*(\theta)}{\left\|\mathbf{a}^{\mathrm{T}}(\theta)\mathbf{U}_{\mathrm{N2}}\mathbf{U}_{\mathrm{N1}}^{\mathrm{H}}\mathbf{a}(\theta)\right\|}. \tag{32}$$

Obviously, in order to make $f(\theta,\beta)$ given in (30) reach the minimum, the negative sign is chosen at the right side of (32). Then, substituting (32) into (30), we have

$$\begin{aligned}f(\theta) &= \mathbf{a}^{\mathrm{H}}(\theta)\mathbf{U}_{\mathrm{N1}}\mathbf{U}_{\mathrm{N1}}^{\mathrm{H}}\mathbf{a}(\theta) + \mathbf{a}(\theta)^{\mathrm{H}}\mathbf{U}_{\mathrm{N2}}\mathbf{U}_{\mathrm{N2}}^{\mathrm{H}}\mathbf{a}(\theta) \\ &\quad - 2\left\|\mathbf{a}^{\mathrm{T}}(\theta)\mathbf{U}_{\mathrm{N2}}\mathbf{U}_{\mathrm{N1}}^{\mathrm{H}}\mathbf{a}(\theta)\right\|.\end{aligned} \tag{33}$$

Meanwhile, it has been proven in [25] that the block matrices $\mathbf{U}_{\mathrm{N1}}$ and $\mathbf{U}_{\mathrm{N2}}$ of noise eigenmatrix $\mathbf{U}_{\mathrm{N}}$ meet the relationship as follows:

$$\mathbf{U}_{\mathrm{N2}} = \mathbf{U}_{\mathrm{N1}}^*\mathbf{\Delta} \tag{34}$$

where $\mathbf{\Delta}$ is a diagonal matrix whose entries are complex numbers with the module of one. Thus, we can obtain the relationship as follows:

$$\mathbf{U}_{\mathrm{N1}}\mathbf{U}_{\mathrm{N1}}^{\mathrm{H}} = \left(\mathbf{U}_{\mathrm{N2}}\mathbf{U}_{\mathrm{N2}}^{\mathrm{H}}\right)^* \tag{35}$$

$$\mathbf{U}_{\mathrm{N2}}\mathbf{U}_{\mathrm{N1}}^{\mathrm{H}} = \left(\mathbf{U}_{\mathrm{N1}}\mathbf{U}_{\mathrm{N2}}^{\mathrm{H}}\right)^*. \tag{36}$$

Substituting (35) and (36) into (33), we can obtain a simplified spatial spectrum function given by

$$f(\theta) = \mathbf{a}^{\mathrm{H}}(\theta)\mathbf{U}_{\mathrm{N1}}\mathbf{U}_{\mathrm{N1}}^{\mathrm{H}}\mathbf{a}(\theta) - \left\|\mathbf{a}^{\mathrm{T}}(\theta)\mathbf{U}_{\mathrm{N2}}\mathbf{U}_{\mathrm{N1}}^{\mathrm{H}}\mathbf{a}(\theta)\right\|. \tag{37}$$

Then, the dimension reduction MUSIC algorithm for maximal noncircularity rated signals (DRNC-MUSIC) is summarized as follows.

Algorithm 1 DRNC-MUSIC algorithm.

1: Estimate covariance matrix $\hat{\mathbf{R}}$ and unconjugated covariance matrix $\hat{\mathbf{R}}'$ using (14) and (18);
2: Construct extended received data vector $\mathbf{y}(t)$ based on (19);
3: Construct the covariance matrix $\mathbf{R}_{\mathbf{y}}$ of extended received data vector $\mathbf{y}(t)$ based on (20);
4: Take the EVD of covariance matrix $\mathbf{R}_{\mathbf{y}}$ based on (26), noise subspace $\mathbf{U}_{\mathrm{N}}$ is obtained;
5: Partition noise subspace $\mathbf{U}_{\mathrm{N}}$ into two block matrices based on (29);
6: Construct spatial spectrum function based on (30);
7: Calculate the partial derivative of $f(\theta,\beta)$ with respect to β and let it be zero, then (31) is obtained;
8: Substitute (32) into (30), the spatial spectrum function of dimension reduction MUSIC algorithm is given by (33);
9: Base on the equation (34), a simplified spatial spectrum function is given by (37).

B. DOA Estimation for Common Noncircularity Rated and Circular Signals

However, in real applications, the form of the signal is not usually simplex; thus, a more generalized algorithm should be proposed to deal with the problem containing more complex signal. In a more specifical way, we should consider the condition that the maximal noncircularity rated and circular signals coexist. It is assumed that there are q incident signals, including q_a maximal noncircularity rated signals and q_b common noncircularity rated and circular signals, and they satisfy $q_a + q_b = q$.

Other related matrices are distinguished based on the subscripts a and b. The former corresponds to maximal noncircularity rated signals, and the later corresponds to common noncircularity rated and circular signals. The signal covariance matrix $\mathbf{R}_{\mathrm{S}}$ can be written as

$$\mathbf{R}_{\mathrm{S}} = \begin{bmatrix} \mathbf{R}_{\mathrm{S}_a} & 0 \\ 0 & \mathbf{R}_{\mathrm{S}_b} \end{bmatrix}. \tag{38}$$

The corresponding manifold matrix can be written as

$$\mathbf{A} = [\mathbf{A}_a \quad \mathbf{A}_b]. \tag{39}$$

Since the noncircularity rated of the maximal noncircularity rated signals satisfies $\rho = 1$, the noncircularity rated and noncircularity phase matrices can be, respectively, expressed as

$$\mathbf{P} = \begin{bmatrix} \mathbf{P}_a & \\ & \mathbf{P}_b \end{bmatrix} = \begin{bmatrix} \mathbf{I}_a & \\ & \mathbf{P}_b \end{bmatrix} \tag{40}$$

$$\mathbf{B} = \begin{bmatrix} \mathbf{B}_a & \\ & \mathbf{B}_b \end{bmatrix}. \tag{41}$$

The extended manifold matrix $\mathbf{A}_{\mathrm{nc}}$ is written as

$$\mathbf{A}_{\mathrm{nc}} = \begin{bmatrix} \mathbf{A}_a & \mathbf{A}_b & -\mathbf{A}_b \\ \mathbf{A}_a^* \mathbf{B}_a^* & \mathbf{A}_b^* \mathbf{B}_b^* & \mathbf{A}_b^* \mathbf{B}_b^* \end{bmatrix} \tag{42}$$

then the extended covariance matrix $\mathbf{R}_{\mathbf{y}}$ can be written as

$$\begin{aligned} \mathbf{R}_{\mathbf{y}} &= \mathbf{A}_{\mathrm{nc}} \begin{bmatrix} \mathbf{R}_{\mathrm{S}_a} & \mathbf{0} & \mathbf{0} \\ \mathbf{0} & \frac{\mathbf{I}_b + \mathbf{B}_b}{2} \mathbf{R}_{\mathrm{S}_b} & \mathbf{0} \\ \mathbf{0} & \mathbf{0} & \frac{\mathbf{I}_b - \mathbf{B}_b}{2} \mathbf{R}_{\mathrm{S}_b} \end{bmatrix} \mathbf{A}_{\mathrm{nc}}^{\mathrm{H}} + \sigma_n^2 \mathbf{I}_{2M} \\ &\triangleq \mathbf{A}_{\mathrm{nc}} \mathbf{R}_{\mathrm{S}_{ab}} \mathbf{A}_{\mathrm{nc}}^{\mathrm{H}} + \sigma_n^2 \mathbf{I}_{2M}. \end{aligned} \tag{43}$$

Based on the orthogonality relationship between manifold matrix $\mathbf{A}_{\mathrm{nc}}$ and noise subspace, we have

$$\mathbf{A}_{\mathrm{nc}}^{\mathrm{H}} \mathbf{U}_{\mathrm{N}} = \begin{bmatrix} \mathbf{A}_a^{\mathrm{H}} & \mathbf{A}_a^{\mathrm{T}} \mathbf{B}_a^{\mathrm{T}} \\ \mathbf{A}_b^{\mathrm{H}} & \mathbf{A}_b^{\mathrm{T}} \mathbf{B}_b^{\mathrm{T}} \\ -\mathbf{A}_b^{\mathrm{H}} & \mathbf{A}_b^{\mathrm{T}} \mathbf{B}_b^{\mathrm{T}} \end{bmatrix} \begin{bmatrix} \mathbf{U}_{\mathrm{N1}} \\ \mathbf{U}_{\mathrm{N2}} \end{bmatrix} = \mathbf{0} \tag{44}$$

i.e.,

$$\begin{cases} \mathbf{A}_a^{\mathrm{H}} \mathbf{U}_{\mathrm{N1}} + \mathbf{A}_a^{\mathrm{T}} \mathbf{B}_a^{\mathrm{T}} \mathbf{U}_{\mathrm{N2}} = \mathbf{0} \\ \mathbf{A}_b^{\mathrm{H}} \mathbf{U}_{\mathrm{N1}} + \mathbf{A}_b^{\mathrm{T}} \mathbf{B}_b^{\mathrm{T}} \mathbf{U}_{\mathrm{N2}} = \mathbf{0} \\ -\mathbf{A}_b^{\mathrm{H}} \mathbf{U}_{\mathrm{N1}} + \mathbf{A}_b^{\mathrm{T}} \mathbf{B}_b^{\mathrm{T}} \mathbf{U}_{\mathrm{N2}} = \mathbf{0}. \end{cases} \tag{45}$$

It can be seen that the steering vector of the maximal noncircularity rated signals satisfies $\mathbf{a}^{\mathrm{H}}(\theta)\mathbf{U}_{\mathrm{N1}} + \mathrm{e}^{\mathrm{j}\phi}\mathbf{a}^{\mathrm{T}}(\theta)\mathbf{U}_{\mathrm{N2}} = \mathbf{0}$. If we construct a spatial spectrum function $f(\theta,\beta) = \|\mathbf{a}^{\mathrm{H}}(\theta)\mathbf{U}_{\mathrm{N1}} + \mathrm{e}^{j\beta}\mathbf{a}^{\mathrm{T}}(\theta)\mathbf{U}_{\mathrm{N2}}\|_{\mathrm{F}}$, the identical form of the simplified spatial spectrum function given in (37) can be obtained. For common noncircularity rated and circular signals, the corresponding steering vectors satisfy

$$\begin{cases} \mathbf{a}^{\mathrm{H}}(\theta)\mathbf{U}_{\mathrm{N1}} + \mathrm{e}^{\mathrm{j}\phi}\mathbf{a}^{\mathrm{T}}(\theta)\mathbf{U}_{\mathrm{N2}} = \mathbf{0}, \\ -\mathbf{a}^{\mathrm{H}}(\theta)\mathbf{U}_{\mathrm{N1}} + \mathrm{e}^{\mathrm{j}\phi}\mathbf{a}^{\mathrm{T}}(\theta)\mathbf{U}_{\mathrm{N2}} = \mathbf{0}. \end{cases} \tag{46}$$

Based on simple calculations, we have

$$\mathbf{a}^{\mathrm{H}}(\theta)\mathbf{U}_{\mathrm{N1}} = \mathbf{0} \tag{47}$$

$$\mathbf{a}^{\mathrm{T}}(\theta)\mathbf{U}_{\mathrm{N2}} = \mathbf{0}. \tag{48}$$

According to (34), the information contained in (47) and (48) is identical. Thus, for common noncircularity rated and circular signals, we can construct a spatial spectrum function as follows:

$$f(\theta,\beta) = \left\|\mathbf{a}^{\mathrm{H}}(\theta)\mathbf{U}_{\mathrm{N1}}\right\|_{\mathrm{F}} = \mathbf{a}^{\mathrm{H}}(\theta)\mathbf{U}_{\mathrm{N1}}\mathbf{U}_{\mathrm{N1}}^{\mathrm{H}}\mathbf{a}(\theta). \tag{49}$$

Then, the dimension reduction MUSIC algorithm for common noncircularity rated and circular signals (DRNC-MUSIC-CC) is summarized as follows.

Algorithm 2 DRNC-MUSIC-CC algorithm.

1: Estimate covariance matrix $\hat{\mathbf{R}}$ and unconjugated covariance matrix $\hat{\mathbf{R}}'$ using (14) and (18);
2: Construct extended received data vector $\mathbf{y}(t)$ based on (19);
3: Construct the covariance matrix $\mathbf{R}_{\mathbf{y}}$ of the extended received data vector $\mathbf{y}(t)$ based on (20);
4: Take the EVD of the covariance matrix $\mathbf{R}_{\mathbf{y}}$ based on (26), the noise subspace $\mathbf{U}_{\mathrm{N}}$ is obtained;
5: Partition the noise subspace $\mathbf{U}_{\mathrm{N}}$ into two block matrices based on (29);
6: Construct the spatial spectrum function based on (49).

For q_b common noncircularity rated and circular signals, we can search the minimum of (49) to achieve the DOAs of

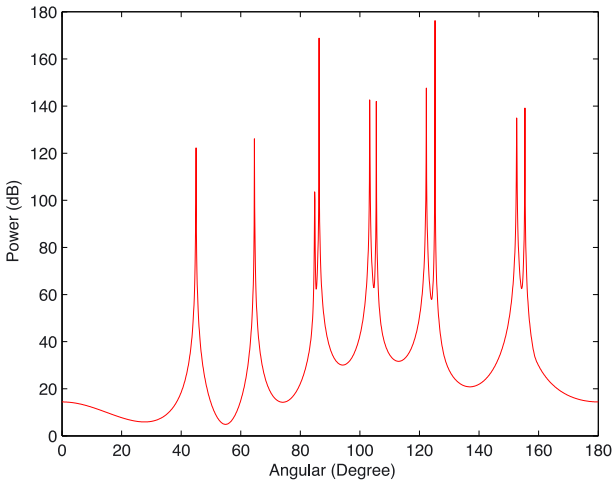

Fig. 1. Pseudopeaking at (85°, 105°, 125°, and 155°) for the common noncircularity rated and circular signals.

incident signals. Compared with (37), we can know that the steering vectors of common noncircularity rated and circular signals given in (47) and (48) make the spatial spectrum function given in (37) equal to zero. It means that the minimum of (37) not only contains the minimum corresponding to DOAs of the maximal noncircularity rated signals but also contains the DOAs of the minimum corresponding to the common noncircularity rated and circular signals. Generally, for common noncircularity rated and circular signals, the estimation accuracy of (49) is better than (37). Then, the information of DOAs of incident signals will be delivered to the data processing center via a wireless sensor network [26], [27].

IV. Discussions

As mentioned previously, the DOAs of the maximal noncircularity rated, common noncircularity rated, and circular signals can be obtained by searching the minimum of (37). However, there exists a problem, i.e., in low SNR, small snapshot numbers, and large source numbers, more than one spectrum peakings may appear in the neighborhoods of DOAs of common noncircularity rated and circular signals in a certain probability. Pseudopeaking may affect DOA estimation for the maximal noncircularity rated signals. An example is shown in Fig. 1. Pseudopeakings appear in (85°, 105°, 125°, and 155°). Six mixed signals impinge on a ULA consisting of six sensors. The directions of two maximal noncircularity rated signals are (45° and 65°), the directions of two common noncircularity rated signals are (85° and 105°), and the directions of two circular signals are (125° and 155°). The SNR is 3 dB, and the snapshot number is 500. The appearance of pseudopeakings will lead to mistake judgment, and the direction finding error would increase.

Then, we will analyze the reason that pseudopeakings may appear in the neighborhoods of DOAs of the common noncircularity rated and circular signals in a certain probability. When (34) is substituted into (37), then (37) can be written as

$$f(\theta) = \mathbf{a}^{\mathrm{H}}(\theta)\mathbf{U}_{\mathrm{N1}}\mathbf{U}_{\mathrm{N1}}^{\mathrm{H}}\mathbf{a}(\theta) - \left\|\mathbf{a}^{\mathrm{T}}(\theta)\mathbf{U}_{\mathrm{N1}}^{*}\Delta\mathbf{U}_{\mathrm{N1}}^{\mathrm{H}}\mathbf{a}(\theta)\right\| \triangleq G_1(\theta) - G_2(\theta). \tag{50}$$

It should be noted that the dimension of matrix $\mathbf{U}_{\mathrm{N1}}$ is $M \times l$, where $l = 2M - q_a - 2q_b \geq 2$. The vectors constructing matrix $\mathbf{U}_{\mathrm{N1}}$ can be expressed as

$$\mathbf{U}_{\mathrm{N1}} = [\mathbf{u}_1, \mathbf{u}_2, \ldots, \mathbf{u}_l]. \tag{51}$$

According to the triangle inequality, we have

$$G_1(\theta) = \sum_{i=1}^{l}\left\|\mathbf{a}^H(\theta)\mathbf{u}_i\right\|^2 = \sum_{i=1}^{l}\left\|\mathrm{e}^{\mathrm{j}\frac{\delta_i}{2}}\left(\mathbf{a}^H(\theta)\mathbf{u}_i\right)^*\right\|^2 \geq \left\|\sum_{i=1}^{l}\mathrm{e}^{\mathrm{j}\delta_i}\left(\mathbf{a}^T(\theta)\mathbf{u}_i^*\right)^2\right\| = G_2(\theta) \tag{52}$$

where $\exp(\mathrm{j}\delta_i), i = 1, 2, \ldots, l$ are the entries of diagonal matrix $\mathbf{\Delta}$. According to the property of inequality, the condition of the equality given in (52) holds when

$$\arg\left(\mathrm{e}^{\mathrm{j}\delta_1}\left(\mathbf{a}^{\mathrm{T}}(\theta)\mathbf{u}_1^*\right)^2\right) = \arg\left(\mathrm{e}^{\mathrm{j}\delta_2}\left(\mathbf{a}^{\mathrm{T}}(\theta)\mathbf{u}_2^*\right)^2\right) = \cdots = \arg\left(\mathrm{e}^{\mathrm{j}\delta_l}\left(\mathbf{a}^{\mathrm{T}}(\theta)\mathbf{u}_l^*\right)^2\right). \tag{53}$$

The function value of each term in (53) would vary continuously when θ varies. The discontinuous hopping points would appear at the locations where the DOAs of common noncircularity rated and circular signals make the modula of each term in (53) equal to zero. Based on the effect of noise and limited sample, the dramatic changes would occur at these discontinuous hopping points. The scope of the dramatic changes will increase when SNR and snapshot number decrease. In the neighborhoods of these angulars, the complex values satisfying (53) would intersect with each other, which would be contained in the minimum by searching (37). Meanwhile, if the equivalent source number becomes smaller, then the value of l would become larger. At this time, the condition of (53) is more critical. Thus, for common noncircularity rated and circular signals, the minimum corresponding to (37) would usually make the modula of each term in (53) achieve minimum. When the equivalent source number becomes larger, then the value of l would become smaller. The points which satisfy or approximately satisfy (53) would appear in the neighborhoods of these discontinuous hopping points. The function value of (37) may become smaller than the minimum of $G_1(\theta)$. Then, pseudopeakings appear in the searching results of (37). In particular, when $l = 2$, i.e., the maximum number of incident signals is achieved, this phenomenon is the most obvious of all.

Based on Fig. 1 and the analysis mentioned previously, in low SNR, small snapshot numbers, and large source numbers, the pseudopeakings would appear in neighborhoods of the spectrum peaking of common noncircularity rated and circular signals. Thus, we can modify (37) by (49). The new spatial spectrum function can be constructed as

$$f(\theta) = \frac{G_1(\theta)G_2(\theta)}{G_1(\theta) - G_2(\theta)} + \frac{1}{\|G_1(\theta)\|_F^2}. \tag{54}$$

In Algorithm 1, (37) can be replaced by (54) to avoid the appearance of pseudopeakings and improve estimation accuracy. This algorithm is called modified DRNC-MUSIC (DRNC-MUSIC-M).

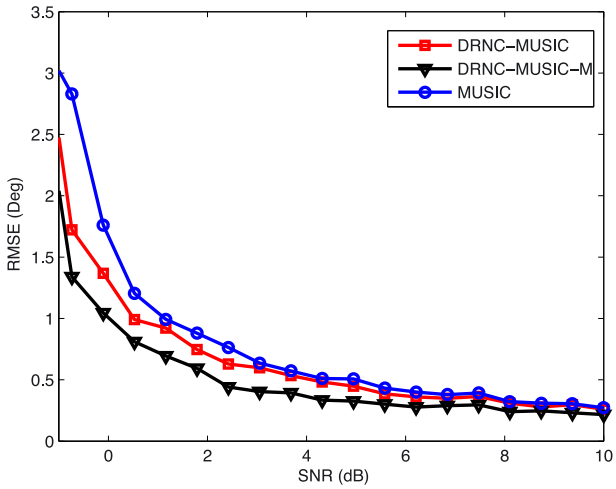

Fig. 2. RMSE versus SNR.

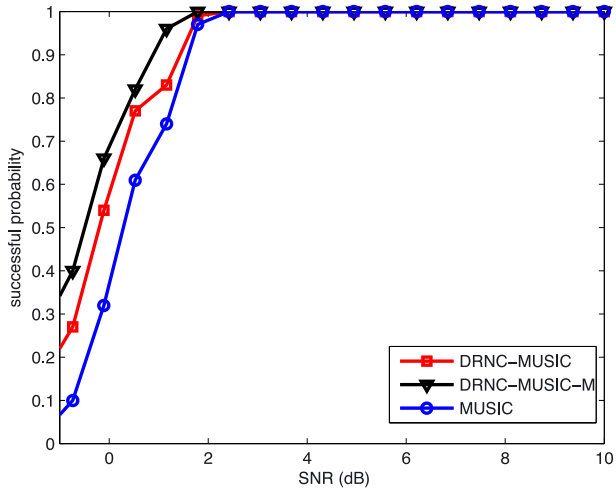

Fig. 3. Successful probability versus SNR.

V. Simulation Results

In this section, numerical results are shown to demonstrate the performances of the proposed algorithms based on MATLAB. A ULA consists of six sensors, and the distance among adjacent sensors is one half-wavelength. CD sources are uncorrelated with each other. Angular spread parameter $\sigma_\theta = 2^\circ$ is identical for all of the CD sources and PDF taken Gaussian distribution for all of the CD sources. We compare the proposed DRNC-MUSIC-M algorithm and DRNC-MUSIC algorithm with the traditional MUSIC algorithm. The number of independent trials is 100. A successful trial is defined as that the difference between the estimated and true DOA is less than 5°. The successful probability is calculated as the ratio between the number of successful trials and the total number of the independent trials.

First, we test the DOA estimation performances of different algorithms versus SNR. The root-mean-square error (rmse) is defined as

$$\text{RMSE} = \sqrt{\frac{1}{N_k}\sum_{k=1}^{N_k}\sum_{i=1}^{q}\left\|\hat{\theta}_i^k - \theta_i\right\|^2} \tag{55}$$

where N_k stands for the number of independent trials and $\hat{\theta}_i^k$ represents the estimated DOA of the ith signal in the kth trial. θ_i represents the true DOA of the ith signal.

It is assumed that one BPSK signal (noncircular one with a noncircularity rate of 1) with direction 35°, two QPSK signals (circular ones a with noncircularity rate of 0) with directions (65° and 85°), and one UQPSK signal (the common noncircularity rated signals) with direction 115° impinge on the ULA. The noncircularity phase of the BPSK signal is 20°, the noncircularity phase of the UQPSK signal is 40°, and the noncircularity rated is 0.5. The snapshot number is fixed at 300. The rmses of different algorithms versus SNRs are depicted in Fig. 2. The successful probabilities of different algorithms versus SNRs are plotted in Fig. 3.

It can be seen from Fig. 2 that the rmse becomes smaller as the SNR increases for all of the algorithms. Due to the application of the unconjugated covariance matrix, more data information is used for DOA estimation for the DRNC-MUSIC algorithm. Thus, the rmse of the DRNC-MUSIC algorithm is smaller than that of the MUSIC algorithm.

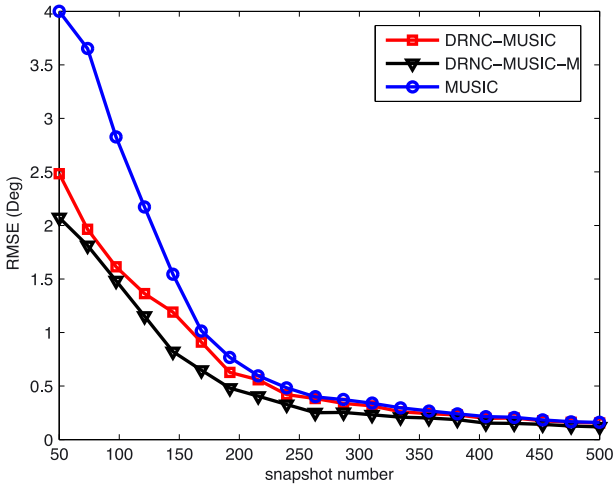

Fig. 4. RMSE versus snapshot number.

However, the DRNC-MUSIC algorithm suffers from the effect of pseudopeakings. The DRNC-MUSIC-M algorithm modifies this drawback. The rmse of the DRNC-MUSIC-M algorithm is smaller than that of the DRNC-MUSIC algorithm.

From Fig. 3, it can be seen that, when the SNR is 3 dB, successful probability approximates to 100%. The successful probability of the DRNC-MUSIC-M algorithm is higher than that of the other two algorithms in a low SNR, which is verified by the results of Fig. 3.

Second, we test the DOA estimation performance of different algorithms versus snapshot number. The SNR is fixed at 3 dB. Other simulation conditions are identical with Fig. 2. The rmses of different algorithms versus snapshot numbers are plotted in Fig. 4. The successful probabilities of different algorithms versus snapshot numbers are plotted in Fig. 5. It can be seen from Fig. 4 that the rmse becomes smaller as the snapshot number increases for all of the algorithms. The proposed DRNC-MUSIC-M algorithm and DRNC-MUSIC algorithm outperform the MUSIC algorithm. Because of the effect of pseudopeakings,

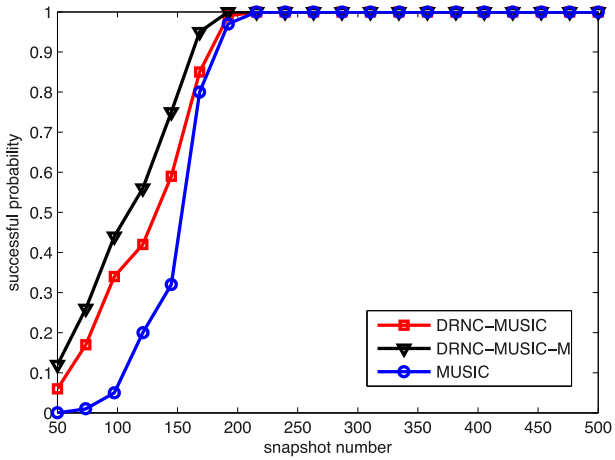

Fig. 5. Spatial spectrums of different algorithms.

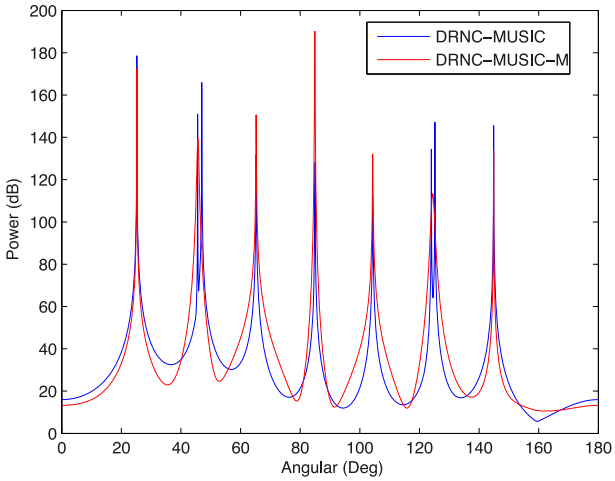

Fig. 6. Successful probability versus snapshot number.

the rmse of the DRNC-MUSIC algorithm is larger than that of the proposed DRNC-MUSIC-M algorithm. For the successful probability shown in Fig. 5, the DRNC-MUSIC-M algorithm outperforms the DRNC-MUSIC algorithm and MUSIC algorithm. This result is identical with the first experiment with respect to SNR.

Finally, we test the condition that the number of incident signals is larger than that of the sensors. At this time, the traditional MUSIC algorithm cannot be used for DOA estimation. Thus, only the DRNC-MUSIC algorithm and DRNC-MUSIC-M algorithm are used for DOA estimation. Seven incident signals impinge on the ULA. The directions of four BPSK signals (noncircular ones with noncircularity rate of 1) are (25°, 65°, 105°, and 145°), and the corresponding noncircularity phases are (10°, 20°, 30°, and 40°), respectively. The directions of two QPSK signals (circular ones with noncircularity rate of 0) are (45° and 85°). One UQPSK signal (the common noncircularity rated signal) with direction 125°, the noncircularity rated, is taken 0.6. The spatial spectrums of these two algorithms are shown in Fig. 6. It can be seen that both of these two algorithms can estimate the DOA of the incident signal accuracy. However, the result of the DRNC-MUSIC algorithm has pseudopeakings. The most obvious angulars are in the neighborhood of (45° and 125°), which correspond to the circular and common noncircularity rated signals, respectively. The proposed DRNC-MUSIC-M algorithm outperforms the DRNC-MUSIC algorithm without pseudopeakings.

VI. Conclusion

In this paper, two MUSIC-like algorithms for CD sources consisting of circular and noncircular signals have been proposed in a massive MIMO system. The maximal noncircularity rated, common noncircularity rated, and circular signals can be estimated synchronously. On imperfect conditions, the pseudopeaking may appear. The reason why pseudopeaking appears is analyzed in detail. The simulation results show that both of the proposed two algorithms can estimate more sources than the number of sensors, which means that more UTs can communicate with BS synchronously. The capacity of BS can increase greatly.

References

[1] J. G. Andrews *et al.*, "What will 5G be?," *IEEE J. Sel. Areas Commun.*, vol. 32, no. 6, pp. 1065–1082, Jun. 2014.
[2] L. Wan, G. Han, J. Rodrigues, W. Si, and N. Feng, "An energy efficient DOA estimation algorithm for uncorrelated and coherent signals in virtual MIMO systems," *Telecommun. Syst.*, vol. 59, no. 1, pp. 93–110, May 2015.
[3] R. Raich, J. Goldberg, and H. Messer, "Bearing estimation for a distributed source: Modeling, inherent accuracy limitations and algorithms," *IEEE Trans. Signal Process.*, vol. 48, no. 2, pp. 429–441, Feb. 2000.
[4] P. Zetterberg, "Mobile cellular communications with base station antenna arrays: Spectrum efficiency, algorithms, and propagation models," Ph.D. Dissertation, Dept. Signal, Sens., Syst., Royal Inst. Technol., Stockholm, Sweden, 1997.
[5] S. Valaee, B. Champagne, and P. Kabal, "Parametric localization of distributed sources," *IEEE Trans. Signal Process.*, vol. 43, no. 9, pp. 2144–2153, Sep. 1995.
[6] R. O. Schmidt, "Multiple emitter location and signal parameter estimation," *IEEE Trans. Antennas Propag.*, vol. 34, no. 3, pp. 276–280, Mar. 1986.
[7] Y. U. Lee, J. Choi, I. Song, and S. R. Lee, "Distributed sources modeling and direction-of-arrival estimation techniques," *IEEE Trans. Signal Process.*, vol. 45, no. 4, pp. 960–969, Apr. 1997.
[8] Y. Zou, H. Xie, L. Wan, and G. Han, "High accuracy frequency and 2D-DOAs estimation of conformal array based on PARAFAC," *J. Internet Technol.*, vol. 16, no. 1, pp. 107–120, Jan. 2015.
[9] L. Wan, G. Han, L. Shu, and N. Feng, "The critical patients localization algorithm using sparse representation for mixed signals in emergency healthcare system," *IEEE Syst. J.*, 2015, to be published. DOI: 10.1109/JSYST.2015.2411745.
[10] O. Besson and P. Stoica, "Decoupled estimation of DOA and angular spread for a spatially distributed source," *IEEE Trans. Signal Process.*, vol. 48, no. 7, pp. 1872–1882, Jul. 2000.
[11] S. Shahbazpanahi, S. Valaee, and M. H. Bastani, "Distributed source localization using ESPRIT algorithm," *IEEE Trans. Signal Process.*, vol. 49, no. 10, pp. 2169–2178, Oct. 2001.
[12] X. S. Guo, Q. Wan, B. Wu, and W. L. Yang, "Parameters localisation of coherently distributed sources based on sparse signal representation," *Inst. Eng. Technol. Radar, Sonar, Navigat.*, vol. 1, no. 4, pp. 261–265, Aug. 2007.
[13] J. Lee, I. Song, H. Kwon, and S. R. Lee, "Low-complexity estimation of 2D DOA for coherently distributed sources," *Signal Process.*, vol. 83, no. 8, pp. 1789–1802, Aug. 2003.
[14] Z. Zhi, G. Li, and Y. Teng, "2D DOA estimator for multiple coherently distributed sources using modified propagator," *Circuits, Syst., Signal Process.*, vol. 31, no. 1, pp. 255–270, Feb. 2012.
[15] P. Gounon, C. Adnet, and J. Galy, "Localisation angulaire de signaux non circulaires," *Trait. Signal*, vol. 15, no. 1, pp. 17–23, 1998.
[16] F. Romer and M. Haardt, "Deterministic Cramer–Rao bounds for strict sense non-circular sources," in *Proc. Int. ITG/IEEE WSA*, Vienna, Austria, 2007, pp. 1–5.

[17] J. P. Delmas, "Asymptotically optimal estimation of DOA for non-circular sources from second order moments," in *Proc. IEEE ICASSP*, Apr. 2003, vol. 5, pp. V.185–V.188.
[18] J. P. Delmas and H. Abeida, "Stochastic Cramer–Rao bound for noncircular signals with application to DOA estimation," *IEEE Trans. Signal Process.*, vol. 52, no. 11, pp. 3192–3199, Nov. 2004.
[19] H. Abeida and J. P. Delmas, "Gaussian Cramer–Rao bound for direction estimation of noncircular signals in unknown noise fields," *IEEE Trans. Signal Process.*, vol. 53, no. 12, pp. 4610–4618, Dec. 2005.
[20] X. Yang, G. Li, Z. Zheng, and L. Zhong, "2D DOA estimation of coherently distributed noncircular sources," *Wireless Pers. Commun.*, vol. 78, no. 2, pp. 1095–1102, Sep. 2014.
[21] A. Hu, T. Lv, H. Gao, Z. Zhang, and S. Yang, "An ESPRIT-based approach for 2D localization of incoherently distributed sources in massive MIMO systems," *IEEE J. Sel. Topics Signal Process.*, vol. 8, no. 5, pp. 996–1011, Oct. 2014.
[22] K. Y. Yang, J. Y. Wu, and W. H. Li, "A low-complexity direction-of-arrival estimation algorithm for full-dimension massive MIMO systems," in *Proc. IEEE ICCS*, Nov. 2014, pp. 472–476.
[23] Y. Zhu, L. Liu, A. Wang, K. Sayana, and J. Zhang, "DOA estimation and capacity analysis for 2D active massive MIMO systems," in *Proc. IEEE ICC*, Jun. 2013, pp. 4630–4634.
[24] Z. T. Huang, Z. M. Liu, J. Liu, and Y. Y. Zhou, "Performance analysis of MUSIC for non-circular signals in the presence of mutual coupling," *Inst. Eng. Technol. Radar, Sonar, Navigat.*, vol. 4, no. 5, pp. 703–711, Oct. 2010.
[25] H. Abeida and J. P. Delmas, "MUSIC-like estimation of direction of arrival for noncircular sources," *IEEE Trans. Signal Process.*, vol. 54, no. 7, pp. 2678–2690, Jul. 2006.
[26] G. Han, J. Jiang, W. Shen, L. Shu, and J. Rodrigues, "IDSEP: A novel intrusion detection scheme based on energy prediction in cluster-based wireless sensor networks," *Inst. Eng. Technol. Inf. Security*, vol. 7, no. 2, pp. 97–105, Jun. 2013.
[27] J. Jiang, G. Han, H. Xu, L. Shu, and M. Guizani, "LMAT: Localization with a mobile anchor node based on trilateration in wireless sensor networks," in *Proc. IEEE GLOBECOM*, Dec. 2011, pp. 1–6.

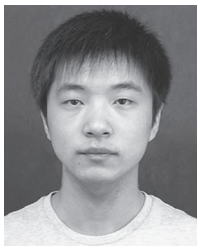

Liangtian Wan (M'15) received the B.S. and Ph.D. degrees from the College of Information and Communication Engineering, Harbin Engineering University, Harbin, China, in 2011 and 2015, respectively.

He is currently a Visiting Scholar with Hohai University, Changzhou, China. His research interests include array signal processing and compressed sensing and its applications.

Dr. Wan has served as a reviewer of over ten journals and TPC member of several international conferences.

Guangjie Han (S'03–M'05) received the Ph.D. degree from Northeastern University, Shenyang, China, in 2004.

From 2004 to 2006, he was a Product Manager with the ZTE Company. In February 2008, he finished his work as a Postdoctoral Researcher with the Department of Computer Science, Chonnam National University, Gwangju, Korea. From October 2010 to 2011, he was a Visiting Research Scholar with Osaka University, Suita, Japan. He is currently a Professor with the Department of Information and Communication System, Hohai University, Nanjing, China. He is the author of over 130 papers published in related international conference proceedings and journals and is the holder of 55 patents. His current research interests include sensor networks, computer communications, mobile cloud computing, and multimedia communication and security.

Dr. Han has served as a Cochair for more than 20 international conferences/workshops and as a Technical Program Committee member of more than 70 conferences. He has served on the editorial boards of up to 16 international journals, including the *International Journal of Ad Hoc and Ubiquitous Computing*, *Journal of Internet Technology*, and *KSII Transactions on Internet and Information Systems*. He has served as a Reviewer of more than 50 journals. He had been awarded the ComManTel 2014, ComComAP 2014, and Chinacom 2014 Best Paper Awards. He is a member of the Association for Computing Machinery.

Jinfang Jiang received the B.S. degree in information and communication engineering from Hohai University, Changzhou, China, in 2009, where she is currently working toward the Ph.D. degree in the Department of Information and Communication System.

Her current research interests are security and localization for sensor networks.

Joel J. P. C. Rodrigues (S'01–M'06–SM'06) received the B.Sc. degree (licentiate) in informatics engineering from the University of Coimbra, Coimbra, Portugal, the M.Sc. degree and the Ph.D. degree in informatics engineering from the University of Beira Interior, Covilhã, Portugal, and the Habilitation from the University of Haute Alsace, Mulhouse, France.

He is a Professor with the Department of Informatics, University of Beira Interior, and a Researcher with the Instituto de Telecomunicações, Portugal. He is the Editor-in-Chief of the *International Journal on E-Health and Medical Communications*, the Editor-in-Chief of the *Recent Advances on Communications and Networking Technology*, and an editorial board member of several journals. He is the author or coauthor of over 350 papers in refereed international journals and conferences, a book, and 3 patents. His main research interests include sensor networks, e-health, e-learning, vehicular delay-tolerant networks, and mobile and ubiquitous computing.

Prof. Rodrigues is the leader of NetGNA Research Group (http://netgna.it.ubi.pt), the Chair of the IEEE ComSoc Technical Committee on eHealth, the Past Chair of the IEEE ComSoc Technical Committee on Communications Software, and a Member Representative of the IEEE Communications Society on the IEEE Biometrics Council. He has been the general chair and TPC chair of many international conferences. He is a member of many international TPCs and has participated in several international conference organizations. He was awarded the 2014 IEEE ComSoc Multimedia Technical Committee Outstanding Leadership Award, the Outstanding Leadership Award of IEEE GLOBECOM 2010 as CSSMA Symposium Cochair, and several best paper awards. He is a licensed professional engineer (as senior member), a member of the Internet Society, an IARIA fellow, and a senior member of ACM.

Naixing Feng received the B.S. degree in electronic science and technology and the M.S. degree in micro-electronics and solid-state electronics from Tianjin Polytechnic University, Tianjin, China, in 2010 and 2013, respectively. He is currently working toward the Ph.D. degree in radio physics at Xiamen University, Xiamen, China.

His current research interests include computational electromagnetics and acoustics.

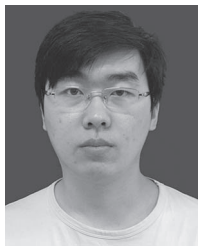

Tong Zhu received the B.S. and Ph.D. degrees from the College of Information and Communication Engineering, Harbin Engineering University, Harbin, China, in 2010 and 2014, respectively.

He is currently a Researcher with Tianjin Institute of Computing Technology, Tianjin, China. His research interests include array signal processing and statistical signal processing.